THE JOURNAL OF PHYSICAL CHEMISTRY C
A JOURNAL OF THE AMERICAN CHEMICAL SOCIETY

pubs.acs.org/JPCC

Article

Sodium Surface Lattice Plasmons

Published as part of The Journal of Physical Chemistry virtual special issue "125 Years of The Journal of Physical Chemistry".

Abdelsalam Rawashdeh, Sylvia Lupa, William Welch, and Ankun Yang*

Cite This: *J. Phys. Chem. C* 2021, 125, 25148–25154

Read Online

ACCESS | Metrics & More | Article Recommendations | Supporting Information

ABSTRACT: Metallic nanostructures can source, detect, and control light through surface plasmons with applications ranging from photocatalysis and biochemical sensors to light trapping in thin-film solar cells. Although the commonly used plasmonic materials such as gold and silver have shown great optical properties, they experience significant ohmic losses that severely limit the device performances. Sodium is predicted to be an ideal plasmonic material with much lower loss than gold and silver across the whole ultraviolet to near-infrared wavelength regime. This paper describes how sodium nanoparticles can exhibit high-quality plasmonic resonances through the excitation of surface lattice plasmons. We investigate both the sodium nanoparticles (size, array period, unit structure) and the excitation light (polarization, angle of incidence) to manipulate how light interacts with sodium nanoparticles. Specifically, by exciting in-plane and out-of-plane surface lattice plasmons, we obtain resonances with extremely narrow line widths and localized electromagnetic field with amplified intensities for sodium nanoparticles. Sodium, as a low-cost and low-loss plasmonic material, provides an affordable alternative in a range of plasmon-enhanced applications such as chemical sensing, thin-film solar cells, and photonic circuits.

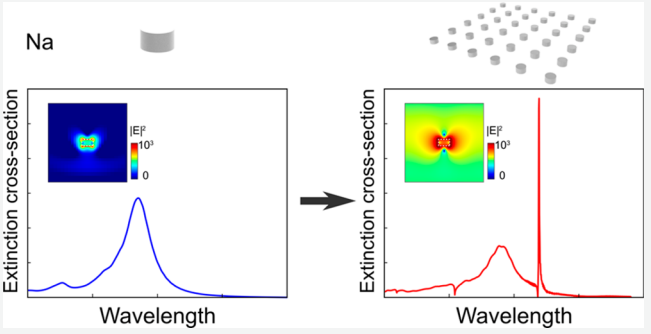

INTRODUCTION

Metallic nanostructures confine free space light into nanoscale dimensions due to their ability to interact with light through surface plasmons.[1] This property enables a strongly localized electromagnetic field with a wide range of applications including biological and chemical sensing,[2−5] surface-enhanced Raman scattering,[6,7] and nanoscale light sources.[8−11] Noble metals such as gold and silver are commonly used plasmonic materials, but they experience parasitic ohmic losses due to electron−phonon and electron−electron scatterings, severely limiting the device performances. Searching for alternative materials with lower loss is an effective strategy to meet the application requirements.[12] Compared with commonly used gold and silver, other researched plasmonic materials include other metals (e.g., aluminum for ultraviolet wavelength[13,14]), metallic alloys,[15] nitrides and oxides,[16,17] etc. Alkali metals, in particular sodium (Na), have long been predicted to be an ideal plasmonic material because they have much lower loss than gold and silver across the whole ultraviolet to near-infrared wavelength regime.[12,18] Sodium experiences lower metal loss due to small intraband optical loss and low electron gas density, both being half that of silver.[18,19] However, due to the chemical reactivity, there has been limited research on Na plasmonics. Recently, a thermo-assisted spin-coating technique taking advantage of the low melting temperature of sodium (98 °C) was used to successfully fabricate Na films.[19] The fabricated Na film exhibited lower optical loss than that of silver over a wide range of wavelengths. In addition, the study has demonstrated that Na-based plasmonic devices can be stable over months with appropriate packaging.[19] Despite the encouraging experimental results on Na films, further advancement requires a fundamental understanding of the optical properties of isolated Na nanoparticles (NPs) to fully assess the potential of Na nanostructures as building blocks in low-loss plasmonic devices. Different from a continuous film that supports propagating electromagnetic waves (surface plasmon polaritons, SPPs), isolated NPs support nonpropagating or localized electron oscillations (localized surface plasmons, LSPs), which do not require momentum matching to be excited as opposed to SPPs. Nanoparticles are the simplest type of plasmonic structure and generally show much lower loss than films because they possess much less material; therefore, they are preferred choices for energy-efficient

Received: June 30, 2021
Revised: October 22, 2021
Published: November 9, 2021

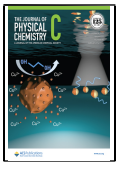

https://doi.org/10.1021/acs.jpcc.1c05833
J. Phys. Chem. C 2021, 125, 25148−25154

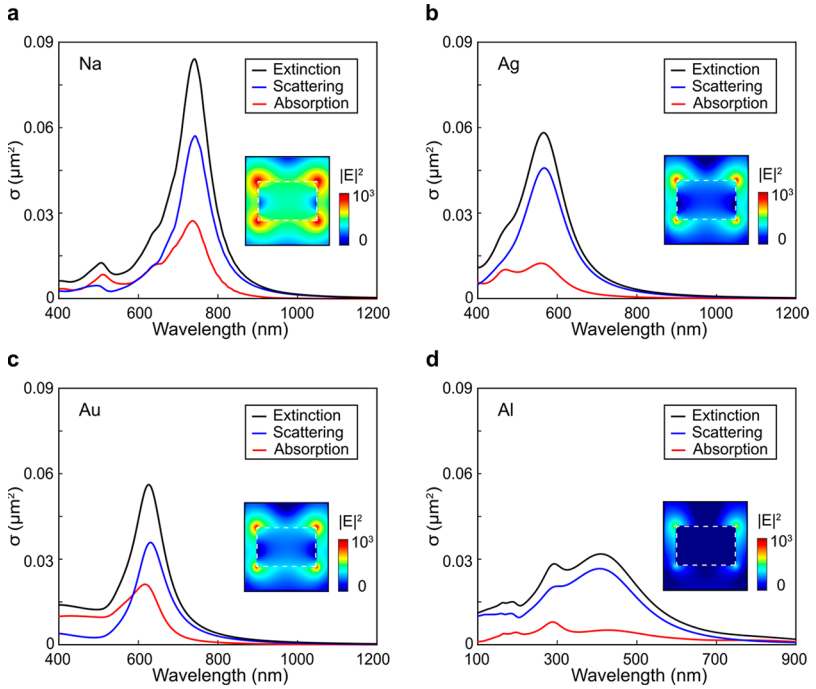

Figure 1. Optical responses of sodium in comparison with other plasmonic materials. Extinction, scattering, and absorption cross sections of (a) Na, (b) Ag, (c) Au, and (d) Al nanoparticles. The dimensions of the nanoparticles are diameter d = 80 nm and height h = 50 nm, outlined with dash lines in the insets, which show the local E-field profiles on resonance.

applications. For example, the LSPs supported by NPs can serve as the cavity modes to stimulate and amplify light emissions for nanoscale lasers.[8]

Single NP LSP resonances, however, generally have large line widths on the order of 100 nm and a low quality factor (Q < 10)[20] due to short plasmon lifetime (2−10 fs).[21] One strategy to improve the Q of LSPs supported by single NPs is arranging these NPs in arrays to establish far-field coupling of the electromagnetic waves associated with LSPs of each NP in the array.[22,23] In contrast to NPs that are randomly distributed where the scattered fields impinging on each NP do not have particular phase relationship, when NPs are arranged in an array with a period similar to the wavelength of the incident light, the scattered fields impinging on a NP can arrive in phase with the incident light. Therefore, the light scattered by each NP into the array can be arranged to be in phase with the plasmon resonance induced in its neighboring NP, using a right combination of NP size, shape, and array period, to reinforce the resonance in the neighboring NP. This strategy can enhance the Q of the resonance and narrow the line width down to a few nanometers.[22−24]

In this paper we theoretically model the optical properties of Na NPs and engineer both the near-field and far-field optical responses of Na NPs through surface lattice plasmons. We show that Na NPs show stronger scattering and absorption cross sections as well as more enhanced local electrical fields (E-field) in comparison with other plasmonic materials due to low imaginary part of the permittivity. Still Na single NPs show broad LSPs due to losses dominated by radiative damping and placing the NPs into an array can effectively suppress the radiative scattering losses leading to narrow surface lattice plasmon resonances. Along with the reduction of the line width (or full-width-at-half-maximum, fwhm), the local electromagnetic fields are also amplified more than ten times that of single Na NPs. We also investigate the ability to engineer optical responses of the Na NPs by changing the unit structure of the array to achieve stronger local electromagnetic field enhancement and polarization-dependent plasmonic properties.

METHODS

Finite-Difference Time-Domain Simulations. FDTD calculations based on commercial software (FDTD solution, Lumerical Inc., Vancouver, Canada) was used to simulate the optical responses of Na, Ag, Au, and Al NPs and NP arrays. The materials data are taken from Wang et al. for Na,[19] Johnson and Christy for Au,[25] and Palik for Ag and Al,[18] respectively. A uniform mesh size of 2 nm (x, y, z directions) was used. To simulate the absorption and scattering cross sections for single NPs and dimers, a total-field scattered-field source was used. To simulate the transmittance and reflectance of the NP and dimer arrays, a plane wave source was used. The boundary conditions were set based on the polarization of the incident light. The dielectric environment was set as n = 1.45. The following equations were used to calculate the extinction (σ_{ext}), scattering (σ_{scat}), and absorption (σ_{abs}) cross sections for the arrays:

$$\sigma_{ext} = (1 - T) \times (p^2 \times \cos\theta) \quad (1)$$

$$\sigma_{scat} = R \times (p^2 \times \cos\theta) \quad (2)$$

$$\sigma_{abs} = (1 - T - R) \times (p^2 \times \cos\theta) \quad (3)$$

where T is transmittance, R is reflectance, p is the array period, and θ is the incident angle.

RESULTS AND DISCUSSION

Figure 1 shows typical optical responses of Na, in comparison with other commonly used plasmonic materials silver (Ag), gold (Au), and aluminum (Al). With the same dimensions

https://doi.org/10.1021/acs.jpcc.1c05833
J. Phys. Chem. C 2021, 125, 25148−25154

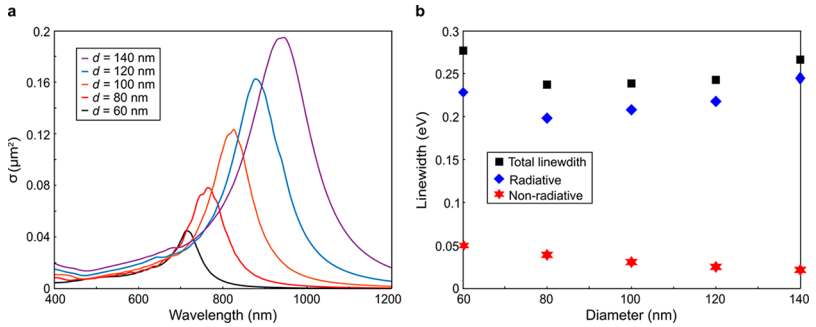

Figure 2. Optical responses of sodium nanoparticles with varying sizes. (a) Extinction cross sections and (b) line width decomposition of Na single NPs as a function of the diameters d = 60−140 nm (height h = 50 nm).

(diameter d = 80 nm, height h = 50 nm), Na exhibits resonances toward the near-infrared while Ag/Au is in the visible and Al is toward the ultraviolet, due to the differences in their bulk plasma frequency (Na, 5.4 eV; Ag, 9.2 eV; Au, 8.9 eV; Al, 12.7 eV).[12,19] Na shows much stronger scattering and absorption cross sections compared with other materials and, due to much lower imaginary part of permittivity (Figure S1), has more enhanced local electrical field (E-field) (maximum $|E|^2/|E_0|^2$ = 1200 for Na, 500 for Ag, 600 for Au, and 100 for Al). We selected the cylindrical shape for comparison because this structure can be potentially fabricated experimentally, e.g., using nanoimprint lithography assisted with heat. We performed size-dependent comparisons of Na versus Ag, a representative plasmonic material with low loss, and found that Na shows higher quality factors (defined as $Q = \lambda/\Delta\lambda$) compared to Ag (Figures S2 and S3).

Figure 2a shows the extinction cross sections of Na single NPs with varying diameters (d = 60−140 nm, h = 50 nm). A single dipolar LSP resonance was observed which red-shifted as a function of the NP diameter from ∼720 nm for the 60 nm NP to ∼930 nm for the 140 nm NP. Although Na NPs generally show much narrower resonances (e.g., in comparison with Ag NPs, Figures S2 and S3), these resonances still show a fwhm >100 nm. The line width of plasmonic resonances can be decomposed into radiative and nonradiative line widths to account for two major line width broadening effects:[26] (1) radiative broadening due to depolarization effects and (2) nonradiative broadening due to electron−phonon interactions, interband transitions, structural defects and surface scattering:

$$\Gamma = \Gamma_{\text{radiative}} + \Gamma_{\text{nonradiative}} \tag{4}$$

Γ is the total line width which can be obtained from the extinction cross sections. $\Gamma_{\text{nonradiative}}$ is the nonradiative line width which can be further written as

$$\Gamma_{\text{nonradiative}} = \Gamma_{\text{bulk}} + \Gamma_{l_{\text{eff}}} \tag{5}$$

where Γ_{bulk} is the line width associated with the dielectric function and the $\Gamma_{l_{\text{eff}}}$ is associated with the electron-surface scattering when the effective path length (l_{eff}) of the electrons is larger than the NPs. For the NPs with $d \geq 60$ nm where l_{eff} is smaller than the NPs (Table S1), we calculate Γ_{bulk} as the main source for nonradiative line width from

$$\Gamma_{\text{bulk}} = \frac{2\,\text{Im}\{\varepsilon\}}{\sqrt{\left(\frac{\partial \text{Re}\{\varepsilon\}}{\partial \omega}\right)^2 + \left(\frac{\partial \text{Im}\{\varepsilon\}}{\partial \omega}\right)^2}} \tag{6}$$

Finally, $\Gamma_{\text{radiative}}$ is determined by eq 4 as

$$\Gamma_{\text{radiative}} = \Gamma - \Gamma_{\text{nonradiative}} \tag{7}$$

In Na NPs, the large line width is dominated by the radiative damping over the nonradiative contributions (Figure 2b). This is consistent with the decomposition of the extinction cross sections into scattering and absorption cross sections where the scattering generally dominates (Figure S4). We also calculated the line width broadening contributed by the surface scattering effect in Na NPs and found their values were actually larger than the nonradiative line width by only considering Γ_{bulk}, possibly due to the small imaginary part of the permittivity of sodium. Nonetheless, the surface scattering induced line width broadening is much smaller than the radiative line width and keeps decreasing as the size of the NP increases (Table S1).

To incorporate plasmonic resonances into applications such as chemical and biological sensing, nanoscale lasing, etc., a narrow resonance (i.e., small fwhm) is desirable. The large radiative line width of Na NPs indicates opportunities to engineer the optical responses through suppressing the radiative scattering. One of the best practices is placing the Na NPs into an ordered array to engineer their optical responses, which has been proven effective in other material systems such as Ag, Au, and Al.[11,14,22−24] Figure 3a shows the transmittance of small Na NPs (e.g., d = 80 nm and h = 50 nm) as a function of the array period. We observe that the resonance approaches the diffractive order as the array period is increased from p = 450 to 600 nm, resulting in a remarkable narrow transmittance peak on the red side of the diffraction edge (Figure 3b). Moreover, the period increment results in narrowing of the resonance with a line width of ∼50 nm (0.1 eV) at the 450 nm period to ∼2 nm (0.003 eV) at the 600 nm period. These narrow resonances are surface lattice plasmon resonances and have been extensively researched in other materials systems.[14,27−31] On these resonances, the scattering cross sections are greatly reduced while the absorption cross sections are enhanced, indicating a suppression of the radiative damping (Figure 3c). These lattice plasmons are excited in the array plane; therefore, they are less sensitive to the height of the NPs. We show that in-plane lattice plasmons can be applied to thicker NPs (e.g., d = 80 nm and h = 100 nm) to achieve much narrower resonances in comparison to the resonances of the single NPs (Figure S5).

For large NPs (e.g., d = 220 nm), high-order lattice plasmons can be excited to exhibit high-quality resonances in the visible to the near-infrared. In this case the LSP continuum is far from the diffraction order and can be seen on the longer-wavelength side of the spectra (Figure 3e,f). However, the high-order modes such as quadrupolar modes can couple into

https://doi.org/10.1021/acs.jpcc.1c05833
J. Phys. Chem. C 2021, 125, 25148−25154

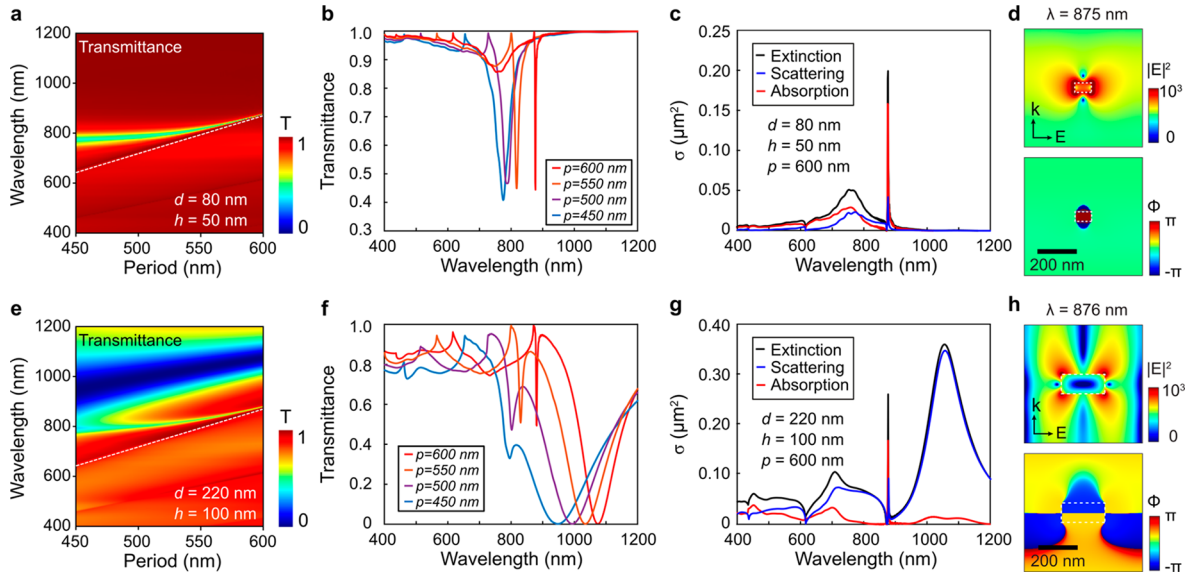

Figure 3. In-plane sodium surface lattice plasmon resonances for small sodium nanoparticles (a–d) and large sodium nanoparticles (e–h). (a, e) Transmittance as a function of the array period of the Na NPs, (b, f) transmittance spectra of Na NPs arranged in arrays with various periods, (c, g) extinction, scattering, and absorption of Na NPs arranged in arrays with p = 600 nm, and (d, h) local electromagnetic field intensity and phase maps. Na NPs in (a–d): d = 80 nm and h = 50 nm. Na NPs in (e–h): d = 220 nm and h = 100 nm.

the diffraction and manifest as narrow surface lattice resonances on the right side of the diffraction order and on the left side of the dipolar LSP. We selected NPs with d = 220 nm and h = 100 nm as an example to show quadrupolar lattice plasmons because NPs with large heights can efficiently separate charges and support high-order modes.[32]

Figure 3d shows the near-field snapshot of the electric field and phase distribution of 80 nm Na NPs with an array period of p = 600 nm at the resonance λ = 875 nm. The near-field phase shows a uniform distribution in and out of the NP, suggesting a dipolar nature of the surface lattice plasmon resonance, which establishes amplified local E-field ($|E|^2/|E_0|^2 = 2 \times 10^4$), much stronger compared to that from a single Na NP ($|E|^2/|E_0|^2$ = 1200, Figure 1a). The electric field snapshot of the 220 nm Na NP (Figure 3h) shows how the electric field is distributed over the four corners of the NP, effectively enhancing the intensity to $|E|^2/|E_0|^2 = 3 \times 10^3$. Moreover, the phase exhibits a 180° difference within the NP indicating a quadrupolar nature of this surface lattice plasmon resonance.[14]

Different from symmetric unit structures such as a cylindrical particle that shows polarization-independent optical responses, a unit structure that has polarization-dependent responses provides an opportunity to tune the surface lattice plasmon resonances simply by the polarization of the incident light. Figure 4 shows an example of using a Na dimer as the unit structure. The Na dimer unit structure shows different LSP resonances when excited either along or perpendicular to the dimer axis (Figure 4b, dashed lines). By sweeping the periods of the lattice, optimized surface lattice plasmon resonances can be achieved independently for both directions (Figure 4b). At the resonance, the local electromagnetic field intensity has the highest value ($|E|^2/|E_0|^2 = 3 \times 10^4$, λ = 1097 nm) when the polarization of light is along the dimer axis, as a result of the strong near-field coupling between the two NPs within the unit as well as the strong far-field coupling among the NPs in the array (Figure 4c). In contrast, the electromagnetic field intensity is weaker for the case when the polarization of light is perpendicular to the dimer axis

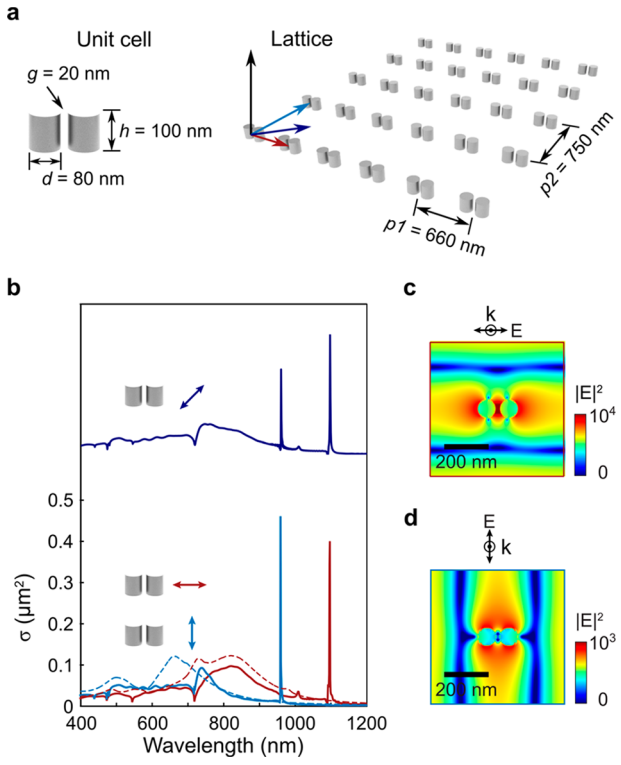

Figure 4. Tunable sodium surface lattice plasmon resonances by unit structure. (a) Schematic of the unit cell and the array of a Na dimer structure. The dimer unit cell has a dimension of diameter d = 80 nm, height h = 100 nm, and gap g = 20 nm. The optimized array periods are $p1$ = 660 nm and $p2$ = 750 nm. (b) Arrays of Na dimers show polarization-dependent surface lattice plasmon resonances. The dashed lines show the optical responses of the single dimer. (c, d) Local electromagnetic field distribution of the dimer under horizontal and vertical polarizations, respectively.

($|E|^2/|E_0|^2 = 1 \times 10^3$, λ = 960 nm) where the enhancement is mainly contributed by the far-field coupling among the NPs

https://doi.org/10.1021/acs.jpcc.1c05833
J. Phys. Chem. C 2021, 125, 25148–25154

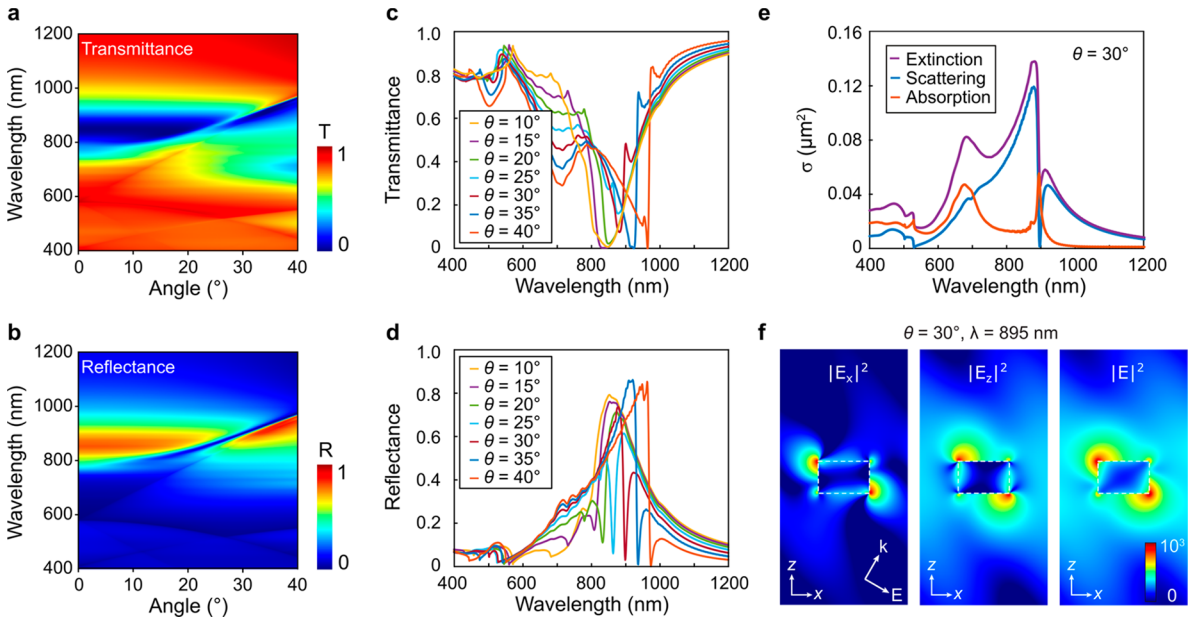

Figure 5. Out-of-plane sodium surface lattice plasmon resonances. (a, b) Transmittance and reflectance of a Na NP array with spacing p = 400 nm, diameter d = 160 nm, and height h = 100 nm. These parameters are optimized to show strong out-of-plane surface lattice plasmon resonances. (c, d) The transmittance and reflectance spectra of the Na NP array at different excitation angles θ = 10°−40°. (e) Extinction, scattering, and absorption cross sections of the Na NP array excited at θ = 30°. (f) The electromagnetic field distribution at the resonance λ = 895 nm showing contributions from both in-plane and out-of-plane excitations.

in the array (Figure 4d). Nonetheless, these enhancement values are much larger in magnitude compared to the enhancement from a single dimer structure with the same dimensions (Figure S6). The independent optimization of the optical responses along different direction is unique and can result in controllable multimodal enhancement potentially useful for parallel biochemical sensing. For example, the 45° polarization results in a mixed response with two high-quality surface lattice plasmon resonances (Figure 4b). Similarly, tuning the polarization direction across 0−360° would result in different ratios of resonance intensities and associated local electromagnetic field enhancement. This idea can be generalized to ellipsoid particles and rectangular particles as unit cell structures.

Besides the in-plane surface lattice plasmon resonances, the incidence angle of light can be controlled to excite out-of-plane surface lattice plasmon resonances to provide another strategy to engineer the optical resonances of the Na NPs. Diameter d = 160 nm, height h = 100 nm, and array period p = 400 nm are the geometrical parameters optimized for the out-of-plane surface lattice plasmon resonance for Na NPs. Figure 5a,b displays the dispersion diagrams for the transmittance and reflectance, respectively. The diffractive modes generated by the NP array cut into the LSP continuum, creating narrow line shapes within broad envelopes (Figure 5c,d). As the angle of excitation is increased from θ = 0° to 40°, the transmittance/reflectance resonances approach the diffractive order, while simultaneously getting narrower to eventually reach the narrowest line width between θ = 25° and 35°. For example, at θ = 30°, the transmittance (reflectance) spectrum of the Na NPs shows a peak (dip) at λ = 895 nm (Figure 5c,d). The line shapes of the out-of-plane surface lattice resonances are very different from those of in-plane surface lattice resonances. At small angles, i.e., ≤20°, the curve takes a bell shape with no obvious sharp peaks/dips. As the angle is increased to >20°, the curve shows an asymmetric peak-and-dip shape that portrays a Fano-type interference between the subradiant out-of-plane lattice plasmon resonance and the in-plane LSP continuum.[21]

We calculated the cross sections and the local electromagnetic field maps at 30° excitation angle (Figure 5e, λ = 895 nm). The extinction cross-section is dominated by the scattering component due to the large size of the NPs. At the resonance, however, the scattering is suppressed while the absorption exhibits a peak. This indicates a strong coupling among the Na NPs that allows one Na NP to re-collect the radiative scattering from its neighboring NPs. With the Fano-type resonances, the extinction and scattering peaks exhibit a much narrower line width compared to that of a single Na NP. In addition, the near-field snapshots (Figure 5f) show that there is local electromagnetic field enhancement in both in-plane $|E_x|^2$ and out-of-plane $|E_z|^2$, contributing to the overall amplified $|E|^2$.

CONCLUSIONS

In this paper we theoretically modeled the optical responses of Na nanoparticles (NPs). We demonstrated several approaches to engineer both far-field resonance line width and local electromagnetic field enhancement for Na NPs through surface lattice plasmons. We show that single Na NPs show stronger scattering and absorption cross sections and more amplified local E-field in comparison to Ag, Au, and Al NPs with the same dimensions but still show broad line widths, which are dominated by radiative damping. By exciting surface lattice plasmons (in-plane and out-of-plane) through the diffractive coupling among the NPs, we show that the radiative scattering can be largely suppressed to yield high-quality surface lattice resonances with narrow line width (~2 nm) and strong local E-field enhancement. By implementing simple unit structures that are sensitive to the polarization of light such as a dimer structure, we achieve surface lattice resonances for both

https://doi.org/10.1021/acs.jpcc.1c05833
J. Phys. Chem. C 2021, 125, 25148−25154

horizontal and vertical polarizations as well as tunable multimodal responses. With surface lattice plasmons, many parameters including the size, shape, array period of NPs, and polarization, and incident angle of light could be controlled to manipulate the optical responses of Na NPs. We anticipate that Na surface lattice plasmons with narrow line widths and amplified local *E*-field can find applications in low-loss plasmonic devices such as photonic integrated circuits, chemical sensing and other solid-state optical devices.

■ ASSOCIATED CONTENT

Supporting Information

The Supporting Information is available free of charge at https://pubs.acs.org/doi/10.1021/acs.jpcc.1c05833.

Dielectric function of sodium in comparison with other plasmonic materials, detailed comparison of optical responses of sodium with silver, decomposition of extinction cross sections of sodium nanoparticles, line width calculations (PDF)

■ AUTHOR INFORMATION

Corresponding Author

Ankun Yang − *Department of Mechanical Engineering, Oakland University, Rochester, Michigan 48309, United States;* orcid.org/0000-0002-0274-4025; Email: ankunyang@oakland.edu

Authors

Abdelsalam Rawashdeh − *Department of Mechanical Engineering, Oakland University, Rochester, Michigan 48309, United States*

Sylvia Lupa − *Department of Mechanical Engineering, Oakland University, Rochester, Michigan 48309, United States*

William Welch − *Department of Mechanical Engineering, Oakland University, Rochester, Michigan 48309, United States*

Complete contact information is available at: https://pubs.acs.org/10.1021/acs.jpcc.1c05833

Notes

The authors declare no competing financial interest.

■ ACKNOWLEDGMENTS

We acknowledge Dr. Jia Zhu from Nanjing University for providing the material data of sodium. Part of the research was supported by the National Science Foundation REU Site program under Grant No. EEC-1852112.

■ REFERENCES

(1) Maier, S. A. *Plasmonics: Fundamentals and Applications*; Springer, 2007.

(2) Anker, J. N.; Hall, W. P.; Lyandres, O.; Shah, N. C.; Zhao, J.; Duyne, R. P. V. Biosensing with Plasmonic Nanosensors. *Nat. Mater.* **2008**, *7* (6), 442−453.

(3) Adato, R.; Yanik, A. A.; Amsden, J. J.; Kaplan, D. L.; Omenetto, F. G.; Hong, M. K.; Erramilli, S.; Altug, H. Ultra-Sensitive Vibrational Spectroscopy of Protein Monolayers with Plasmonic Nanoantenna Arrays. *Proc. Natl. Acad. Sci. U. S. A.* **2009**, *106* (46), 19227−19232.

(4) Kinkhabwala, A.; Yu, Z.; Fan, S.; Avlasevich, Y.; Müllen, K.; Moerner, W. E. Large Single-Molecule Fluorescence Enhancements Produced by a Bowtie Nanoantenna. *Nat. Photonics* **2009**, *3* (11), 654−657.

(5) Shen, Y.; Zhou, J.; Liu, T.; Tao, Y.; Jiang, R.; Liu, M.; Xiao, G.; Zhu, J.; Zhou, Z.-K.; Wang, X.; et al. Plasmonic Gold Mushroom Arrays with Refractive Index Sensing Figures of Merit Approaching the Theoretical Limit. *Nat. Commun.* **2013**, *4*, 4.

(6) Haynes, C. L.; Duyne, R. P. V. Plasmon-Sampled Surface-Enhanced Raman Excitation Spectroscopy †. *J. Phys. Chem. B* **2003**, *107* (30), 7426−7433.

(7) Nie, S.; Emory, S. R. Probing Single Molecules and Single Nanoparticles by Surface-Enhanced Raman Scattering. *Science* **1997**, *275* (5303), 1102−1106.

(8) Noginov, M. A.; Zhu, G.; Belgrave, A. M.; Bakker, R.; Shalaev, V. M.; Narimanov, E. E.; Stout, S.; Herz, E.; Suteewong, T.; Wiesner, U. Demonstration of a Spaser-Based Nanolaser. *Nature* **2009**, *460* (7259), 1110−1112.

(9) Oulton, R. F.; Sorger, V. J.; Zentgraf, T.; Ren−Min, M.; Gladden, C.; Dai, L.; Bartal, G.; Zhang, X. Plasmon Lasers at Deep Subwavelength Scale. *Nature* **2009**, *461* (7264), 629−632.

(10) Zhou, W.; Dridi, M.; Suh, J. Y.; Kim, C. H.; Co, D. T.; Wasielewski, M. R.; Schatz, G. C.; Odom, T. W. Lasing Action in Strongly Coupled Plasmonic Nanocavity Arrays. *Nat. Nanotechnol.* **2013**, *8* (7), 506−511.

(11) Yang, A.; Hoang, T. B.; Dridi, M.; Deeb, C.; Mikkelsen, M. H.; Schatz, G. C.; Odom, T. W. Real-Time Tunable Lasing from Plasmonic Nanocavity Arrays. *Nat. Commun.* **2015**, *6*, 6939.

(12) West, P. R.; Ishii, S.; Naik, G. V.; Emani, N. K.; Shalaev, V. M.; Boltasseva, A. Searching for Better Plasmonic Materials. *Laser & Photonics Reviews* **2010**, *4* (6), 795−808.

(13) Knight, M. W.; King, N. S.; Liu, L.; Everitt, H. O.; Nordlander, P.; Halas, N. J. Aluminum for Plasmonics. *ACS Nano* **2014**, *8* (1), 834−840.

(14) Yang, A.; Hryn, A. J.; Bourgeois, M. R.; Lee, W.-K.; Hu, J.; Schatz, G. C.; Odom, T. W. Programmable and Reversible Plasmon Mode Engineering. *Proc. Natl. Acad. Sci. U. S. A.* **2016**, *113* (50), 14201−14206.

(15) Blaber, M. G.; Arnold, M. D.; Ford, M. J. A Review of the Optical Properties of Alloys and Intermetallics for Plasmonics. *J. Phys.: Condens. Matter* **2010**, *22* (14), 143201.

(16) Naik, G. V.; Schroeder, J. L.; Ni, X.; Kildishev, A. V.; Sands, T. D.; Boltasseva, A. Titanium Nitride as a Plasmonic Material for Visible and Near-Infrared Wavelengths. *Opt. Mater. Express* **2012**, *2* (4), 478.

(17) Li, S.-Q.; Guo, P.; Buchholz, D. B.; Zhou, W.; Hua, Y.; Odom, T. W.; Ketterson, J. B.; Ocola, L. E.; Sakoda, K.; Chang, R. P. H. Plasmonic-Photonic Mode Coupling in Indium-Tin-Oxide Nanorod Arrays. *ACS Photonics* **2014**, *1* (3), 163−172.

(18) Palik, E. D. *Handbook of Optical Constants of Solids*; Academic, 1985.

(19) Wang, Y.; Yu, J.; Mao, Y.-F.; Chen, J.; Wang, S.; Chen, H.-Z.; Zhang, Y.; Wang, S.-Y.; Chen, X.; Li, T.; et al. Stable, High-Performance Sodium-Based Plasmonic Devices in the near Infrared. *Nature* **2020**, *581* (7809), 401−405.

(20) Lilley, G.; Messner, M.; Unterrainer, K. Improving the Quality Factor of the Localized Surface Plasmon Resonance. *Opt. Mater. Express* **2015**, *5* (10), 2112−2120.

(21) Zhou, W.; Odom, T. W. Tunable Subradiant Lattice Plasmons by Out-of-Plane Dipolar Interactions. *Nat. Nanotechnol.* **2011**, *6* (7), 423−427.

(22) Zou, S.; Schatz, G. C. Narrow Plasmonic/Photonic Extinction and Scattering Line Shapes for One and Two Dimensional Silver Nanoparticle Arrays. *J. Chem. Phys.* **2004**, *121* (24), 12606−12612.

(23) Zou, S.; Janel, N.; Schatz, G. C. Silver Nanoparticle Array Structures That Produce Remarkably Narrow Plasmon Lineshapes. *J. Chem. Phys.* **2004**, *120* (23), 10871−10875.

(24) Kravets, V. G.; Kabashin, A. V.; Barnes, W. L.; Grigorenko, A. N. Plasmonic Surface Lattice Resonances: A Review of Properties and Applications. *Chem. Rev.* **2018**, *118* (12), 5912−5951.

(25) Johnson, P. B.; Christy, R. W. Optical Constants of the Noble Metals. *Phys. Rev. B* **1972**, *6*, 4370.

(26) Ross, M. B.; Schatz, G. C. Radiative Effects in Plasmonic Aluminum and Silver Nanospheres and Nanorods. *J. Phys. D: Appl. Phys.* **2015**, *48* (18), 184004.
(27) Wang, D.; Yang, A.; Hryn, A. J.; Schatz, G. C.; Odom, T. W. Superlattice Plasmons in Hierarchical Au Nanoparticle Arrays. *ACS Photonics* **2015**, *2*, 1789−1794.
(28) Vecchi, G.; Giannini, V.; Rivas, J. G. Surface Modes in Plasmonic Crystals Induced by Diffractive Coupling of Nanoantennas. *Phys. Rev. B: Condens. Matter Mater. Phys.* **2009**, *80* (20), 201401.
(29) Kravets, V.; Schedin, F.; Grigorenko, A. Extremely Narrow Plasmon Resonances Based on Diffraction Coupling of Localized Plasmons in Arrays of Metallic Nanoparticles. *Phys. Rev. Lett.* **2008**, *101* (8), 087403.
(30) Auguié, B.; Barnes, W. Collective Resonances in Gold Nanoparticle Arrays. *Phys. Rev. Lett.* **2008**, *101* (14), 143902.
(31) Chu, Y.; Schonbrun, E.; Yang, T.; Crozier, K. B. Experimental Observation of Narrow Surface Plasmon Resonances in Gold Nanoparticle Arrays. *Appl. Phys. Lett.* **2008**, *93* (18), 181108−181108.
(32) Wang, D.; Bourgeois, M. R.; Lee, W.-K.; Li, R.; Trivedi, D.; Knudson, M. P.; Wang, W.; Schatz, G. C.; Odom, T. W. Stretchable Nanolasing from Hybrid Quadrupole Plasmons. *Nano Lett.* **2018**, *18* (7), 4549−4555.

https://doi.org/10.1021/acs.jpcc.1c05833
J. Phys. Chem. C 2021, 125, 25148−25154